Intracellular calcium transients evoked by pulsed infrared radiation in neonatal cardiomyocytes

Gregory M. Dittami[1], Suhrud M. Rajguru[1,2], Richard A. Lasher[1], Robert W. Hitchcock[1] and Richard D. Rabbitt[1,3,4]

[1]*Department of Bioengineering, University of Utah, Salt Lake City, UT 84112, USA*
[2]*Department of Otolaryngology, Northwestern University, Chicago, IL 60611, USA*
[3]*Marine Biological Laboratory, Woods Hole, MA 02543, USA*
[4]*Otolaryngology, Head & Neck Surgery, University of Utah, Salt Lake City, UT 84112, USA*

Non-technical summary We have investigated the mechanisms underlying the response of cells to pulsed infrared radiation (IR, ∼1862 nm) using the neonatal rat ventricular cardiomyocyte as a model. Fluorescence monitoring of the intracellular free calcium (Ca^{2+}) demonstrated that infrared irradiation induced rapid (millisecond time scale) intracellular Ca^{2+} transients in the cells. The results showed that the Ca^{2+} transients were sufficient to elicit contractile responses from the cardiomyocytes and could be 'paced' or entrained to the pulsing frequency of the IR. Pharmacological results strongly implicate mitochondria as the primary intracellular organelles contributing to the IR-evoked Ca^{2+} cycling.

Abstract Neonatal rat ventricular cardiomyocytes were used to investigate mechanisms underlying transient changes in intracellular free Ca^{2+} concentration ($[Ca^{2+}]_i$) evoked by pulsed infrared radiation (IR, 1862 nm). Fluorescence confocal microscopy revealed IR-evoked $[Ca^{2+}]_i$ events with each IR pulse (3–4 ms pulse^{-1}, 9.1–11.6 J cm^{-2} pulse^{-1}). IR-evoked $[Ca^{2+}]_i$ events were distinct from the relatively large spontaneous $[Ca^{2+}]_i$ transients, with IR-evoked events exhibiting smaller amplitudes (0.88 $\Delta F/F_0$ *vs.* 1.99 $\Delta F/F_0$) and shorter time constants ($\tau = 0.64$ s *vs.* 1.19 s, respectively). Both IR-evoked $[Ca^{2+}]_i$ events and spontaneous $[Ca^{2+}]_i$ transients could be entrained by the IR pulse (0.2–1 pulse s^{-1}), provided the IR dose was sufficient and the radiation was applied directly to the cell. Examination of IR-evoked events during peak spontaneous $[Ca^{2+}]_i$ periods revealed a rapid drop in $[Ca^{2+}]_i$, often restoring the baseline $[Ca^{2+}]_i$ concentration, followed by a transient increase in $[Ca^{2+}]_i$. Cardiomyocytes were challenged with pharmacological agents to examine potential contributors to the IR-evoked $[Ca^{2+}]_i$ events. Three compounds proved to be the most potent, reversible inhibitors: (1) CGP-37157 (20 μM, $n = 12$), an inhibitor of the mitochondrial Na^+/Ca^{2+} exchanger (mNCX), (2) Ruthenium Red (40 μM, $n = 13$), an inhibitor of the mitochondrial Ca^{2+} uniporter (mCU), and (3) 2-aminoethoxydiphenylborane (10 μM, $n = 6$), an IP_3 channel antagonist. Ryanodine blocked the spontaneous $[Ca^{2+}]_i$ transients but did not alter the IR-evoked events in the same cells. This pharmacological array implicates mitochondria as the major intracellular store of Ca^{2+} involved in IR-evoked responses reported here. Results support the hypothesis that 1862 nm pulsed IR modulates mitochondrial Ca^{2+} transport primarily through actions on mCU and mNCX.

(Received 30 August 2010; accepted after revision 11 January 2011; first published online 17 January 2011)
Corresponding author G. M. Dittami: Biomedical Polymers Research Building, 20 S 2030 E, Room 108, Salt Lake City, UT 84112, USA. Email: dittami@eng.utah.edu

Abbreviations CICR, calcium induced calcium release; ECC, excitation–contraction coupling; ER, endoplasmic reticulum; IR, infrared radiation; mCU, mitochondrial calcium uniporter; mNCX, mitochondrial sodium/calcium exchanger; RyR, ryanodine receptor; SERCA, sarco/endoplasmic reticulum ATPase; SR, sarcoplasmic reticulum.

DOI: 10.1113/jphysiol.2010.198804

Introduction

Intracellular Ca^{2+} signalling plays a fundamental role in virtually all excitable cells, and is perhaps most clearly demonstrated by the control of synaptic release in neurons and by active contraction in cardiomyocytes. The importance of excitability to therapeutics and basic science has motivated examination of chemical, electrical and optical stimuli in the hope of identifying effective means to extrinsically manipulate cells. Recent evidence suggests that short pulses of infrared radiation (IR) evoke controllable cytosolic $[Ca^{2+}]$ transients (Smith *et al.* 2001; Tseeb *et al.* 2009). In fact, IR has been shown to excite cells under a variety of conditions, both *in situ* and *in vivo*. Long-wavelength, pulsed IR laser radiation (∼1800–2120 nm), *in vivo*, evokes responses in rat sciatic nerve (Wells *et al.* 2005), auditory nerve (Izzo *et al.* 2006), quail embryo hearts (Jenkins *et al.* 2010) and vestibular hair cells (Rajguru *et al.* 2011); and pulsed IR (750–850 nm), *in vitro*, evokes responses in HeLa cells (Smith *et al.* 2001), pyramidal neurons (Hirase *et al.* 2002), PC12 cells (Smith *et al.* 2006), neonatal cardiomyocytes (Smith *et al.* 2008) and astrocytes (Zhao *et al.* 2009). Whether an IR-evoked Ca^{2+} signal led to excitation or some other key signal was at play is not known. The present study was designed to examine the origin(s) of pulsed, 1862 nm, IR-evoked $[Ca^{2+}]$ transients and IR excitability with specific attention to responses in isolated cardiomyocytes.

Early work in optical radiation of excitable cells attributed responses to depolarization caused by light interaction with intracellular chromophores (Arvanitaki & Chalazonitis, 1961). Results using direct and indirect pulsed lasers suggest that thermal effects are very important (Wells *et al.* 2007; Tseeb *et al.* 2009), and override effects of pressure, electric fields or photochemistry (Wells *et al.* 2007). Studies using IR at 780 nm, identified IR-evoked release, and subsequent Ca^{2+} wave propagation' as the primary observable cellular response (Smith *et al.* 2001; Iwanaga *et al.* 2006). The probability of $[Ca^{2+}]_i$ wave propagation was unaffected by removal of extracellular Ca^{2+} and was decreased by the application of thapsigargin, a sarco/endoplasmic reticulum Ca^{2+}-ATPase (SERCA), inhibitor, indicating an intracellular release origin and a subsequent role for endoplasmic reticulum (ER) in the amplification of the $[Ca^{2+}]_i$ signal (Iwanaga *et al.* 2006). Furthermore, focusing the IR to subcellular regions distinguished between IR stimulation of the cytoplasm and IR stimulation of the plasma membrane. The former evoked membrane hyperpolarizations and the latter evoked transient depolarizations followed by slower repolarizations (Ando *et al.* 2009). While the hyperpolarization effects were attributed to a secondary effect of the $[Ca^{2+}]_i$ release on Ca^{2+}-activated potassium channels, the depolarization was hypothesized to have resulted from direct IR-induced membrane perforations. Responses to heat pulses in the absence of direct IR have also been investigated previously in HeLa cells (Tseeb *et al.* 2009). Heat pulses were applied using 1064 nm pulsed IR applied to aluminium nanoparticles adjacent to the cell. Because heat-pulse evoked $[Ca^{2+}]_i$ transients were blocked by thapsigargin (Tseeb *et al.* 2009), it was suggested that the heat pulse stimulus resulted in SERCA uptake into ER. As addition of histamine, an inositol trisphosphate (IP_3)-channel antagonist, blocked $[Ca^{2+}]_i$ release, it was further hypothesized that rapid cooling led to IP_3-channel release from ER, resulting in a $[Ca^{2+}]_i$ 'overshoot' or transient increase.

The present study examines mechanisms underlying $[Ca^{2+}]_i$ transients evoked by direct application of 1862 nm pulsed IR. Cardiomyocytes were identified as a model cell line for their vigorous (up to 1 μM $[Ca^{2+}]_i$ during spontaneous transients), easily imaged Ca^{2+} induced Ca^{2+} release (CICR) associated with excitation–contraction coupling (ECC) (Cannell *et al.* 1987; Bers, 2008). Neonatal rat ventricular cardiomyocytes, specifically, were chosen to facilitate maintenance in culture. As stimulation of cardiomyocytes with IR near 1862 nm has not been previously reported, initial experiments were performed to determine the viability of the approach as well as the radiant energy threshold required to evoke $[Ca^{2+}]_i$ events. IR-evoked $[Ca^{2+}]_i$ events were subsequently compared to spontaneous $[Ca^{2+}]_i$ transients. Finally, key contributors to the IR-evoked $[Ca^{2+}]_i$ events were examined pharmacologically.

Methods

Cardiomyocyte isolation and culture

All animal procedures were approved by the University of Utah Institutional Animal Use and Care Committee and comply with policies and regulations of *The Journal of Physiology* (Drummond, 2009). Rat ventricular cardiomyocytes were harvested from 1–2 day postnatal Sprague–Dawley rats (Charles River Laboratories, Wilmington, MA, USA) following an established protocol and using a neonatal cardiomyocyte isolation kit from Worthington Biochemical (Lakewood, NJ, USA). Briefly, neonatal rats were anaesthetized with isofluorane inhalation and killed by decapitation. Hearts were immediately and aseptically removed. Ventricles were separated from the atria and collected in Ca^{2+}- and magnesium-free Hanks' balanced salt solution (HBSS). Ventricles were finely minced and digested in 50 μg ml^{-1} trypsin at 4°C overnight. Further digestion was performed the following day with collagenase (1500 units) in Leibovitz L-15 medium. Cell suspensions were triturated, filtered, centrifuged and resuspended in culture medium

(Dulbecco's modified Eagle's medium (DMEM)–F12 supplemented with 10% equine serum, 1% L-glutamine, 20 units ml^{-1} penicillin, and 20 mg ml^{-1} streptomycin). Myocytes were enriched by depleting the fibroblasts through 30–45 min of differential pre-plating at 37°C (adapted from Fink *et al.* 2000). Non-adherent cells (myocytes) were pelleted, re-suspended, and plated in culture medium on poly-DL-lysine (P4158, Sigma-Aldrich Corp., St Louis, MO, USA) coated polystyrene culture dishes at a density of ∼25,000 cells cm^{-2}. Dishes were maintained in an incubator at 37°C with 5% CO_2. Medium was refreshed every 3–4 days. Cells used in experiments were taken 7–21 days post-isolation.

Fluo-4 AM loading and Ca^{2+} imaging

Prior to cell use, culture medium was replaced with modified Tyrode solution consisting of 140 mM NaOH, 10 mM glucose, 10 mM Hepes, 4 mM KCl, 1 mM $MgCl_2$, and 1.8 mM $CaCl_2$ (pH adjusted to 7.4 with NaOH). Cells were loaded for 45 min at 37°C with 4–6 μM Fluo-4 AM (Invitrogen, Carlsbad, CA, USA) dye containing 0.1% Pluronic F-127 (Invitrogen). Following dye loading, cells were washed with fresh modified Tyrode solution and further incubated for 15 min at room temperature to allow for full acetoxymethyl (AM) ester cleavage.

Imaging was performed at room temperature on a confocal microscope (FV 1000, Olympus America, Centre Valley, PA, USA) with a water-immersion objective (40× LUMPlanFL N, Olympus America). Time-series scans, with 256 × 256 pixels $frame^{-1}$ resolution, were taken in roundtrip scanning mode with a pixel dwell time of 0.5 μs thereby achieving a frame rate (0.129 s or less with region of interest (ROI) specification) sufficient to resolve the IR-evoked $[Ca^{2+}]_i$ transient events. An argon laser was used for excitation (488 nm, 3% power) and emissions were collected between 500 nm and 600 nm. Image sequences were collected and converted into individual TIFF files with the Fluoview imaging software (Olympus) along with the imaging parameters file.

Pulsed infrared stimulation

A Capella pulsed IR laser source (Lockheed Martin Aculight, Bothell, WA, USA) coupled to a low-OH, 400 μm diameter optical fibre (Ocean Optics, Dunedin, FL, USA) was used to deliver the IR to the cardiomyocytes. The output fibre was mounted into a micromanipulator and visually positioned within 300 μm of the targeted myocytes by observing the fibre-delivered pilot light illumination (visible red) of the cells with the microscope in transmission illumination mode. The output wavelength and power percentage were set to 1862 nm and 100%, respectively, for all experiments. The choice of 1862 nm derives from earlier work demonstrating the promise of this approximate wavelength (1.87 μm) in rat sciatic nerve (Wells *et al.* 2007). The same wavelength has also been shown to safely stimulate cochlear spiral ganglion at 200 Hz for up to 10 h in cat cochleae (Rajguru *et al.* 2010). Activation threshold analysis was performed *post hoc* through analysis of cell exposure data with pulse widths ranging from 1.75 ms $pulse^{-1}$ to 4.0 ms $pulse^{-1}$. This corresponded to calculated radiant exposures, assuming a spot size diameter of 400 μm, of 5.1 J cm^{-2} to 11.6 J cm^{-2}. For all other experiments, pulse widths of 3–4 ms (9.1–11.6 J cm^{-2}) were applied. Radiant energy output at the fibre tip was measured using a 3Sigma meter with a PS19Q sensor (Coherent, Santa Clara, CA, USA). Triggering of pulse delivery was accomplished either manually or automatically (0.25–1 pulses s^{-1}) using the internal clock of the laser source. For manually triggered pulsing, the keyboard-activated, software-triggered TTL output from the FV1000 microscope was used as the external TTL input to the laser.

Pharmacological studies

2-Aminoethoxydiphenylborane (2-APB; 10 μM), 7-chloro-5-(2-chlorophenyl)-1,5-dihydro-4,1-benzothiazepin-2(3*H*)-one (CGP-37157; 20 μM) and ryanodine (100 μM) from Tocris Bioscience (Ellisville, MO, USA) were dissolved in dimethylsulfoxide (DMSO) at 1000 times the final-dose concentrations, aliquoted into single-dose containers, and stored at –20°C until use. In addition, Ruthenium Red (40 μM, Sigma-Aldrich) was prepared fresh on the day of the experiment in modified Tyrode solution in concentrations 1000 times the final dose. Prior to application, all drugs were diluted in 0.5 ml modified Tyrode solution. Final drug delivery was accomplished through pipettes that were positioned over the cell(s). Fluorescence recordings in the presence of the drugs were taken roughly 10–15 min post-addition. Following drug treatment, cells were washed four times thereby replacing the entire dish volume with drug-free Tyrode solution for a total of roughly 12 ml of wash solution.

Image processing

Post-processing of the image sequences was performed using a custom-coded program (Igor Pro, WaveMetrics, Lake Oswego, OR, USA). Relative fluorescence intensities were averaged over each region of interest (ROI) for each frame. All fluorescence intensities were reported as $\Delta F/F_0$ where $\Delta F = F_r - F_0$, F_r is the recorded (absolute) intensity value, and F_0 is the average baseline intensity of the cell during quiescence (no IR stimulation and cell resting periods). Firing rates for cells during synchronization experiments were calculated as

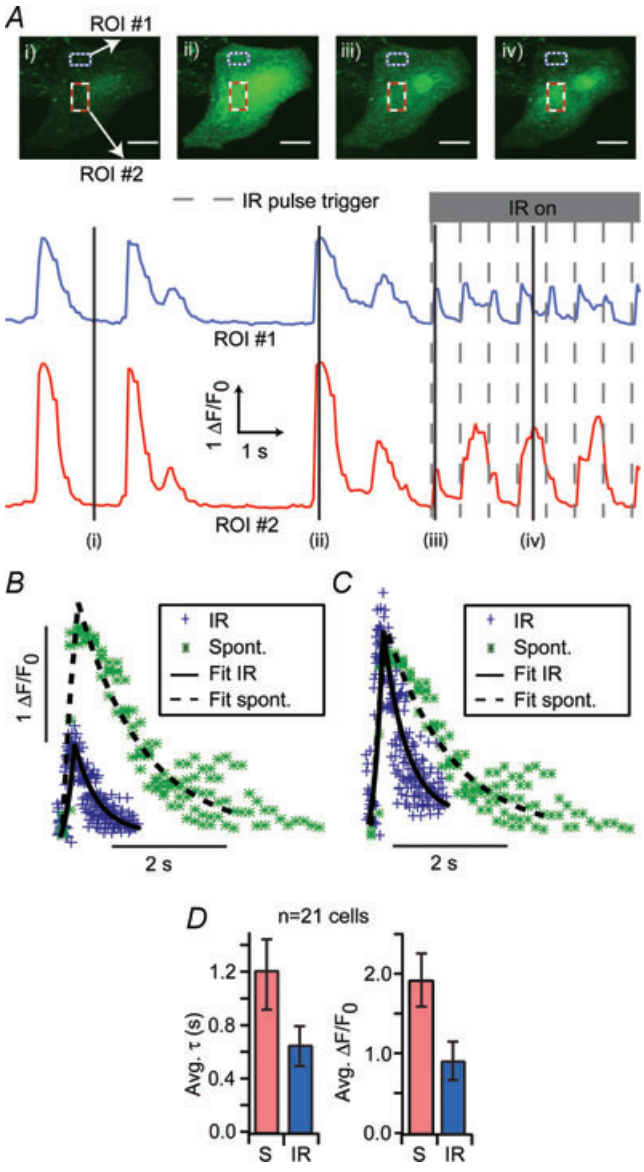

Figure 1. IR – evoked *vs.* spontaneous Ca^{2+} release
A, fluorescence images of a fluo-4 AM (4 μM) loaded neonatal cardiomyocyte during rest (*i*), spontaneous $[Ca^{2+}]_i$ transient (*ii*), IR-evoked $[Ca^{2+}]_i$ increase (*iii*) and a Ca^{2+} spark event (*iv*). White scale bars are 20 μm in length. $[Ca^{2+}]_i$ fluorescence intensity plots for each of the boxed, regions of interest (ROIs) in the cells (top/blue and a bottom/red rectangles). Markers indicate the corresponding image locations on the fluorescence traces. *B*, averaged transient data for the cell from *A* were plotted and fitted with a double exponential rise and exponential decay. *C*, average transient data scaled to show temporal differences. *D*, similar fits were performed and aggregated for 21 cells. Curves could be fitted with similar rise time constants but the time constant for exponential decay (τ) of the IR-evoked events ('IR', $\tau = 0.64 \pm 0.14$ s) was roughly half that of the spontaneous response ('S', $\tau = 1.19 \pm 0.25$ s). IR evoked $[Ca^{2+}]_i$ event amplitudes (0.88 ± 0.23 $\Delta F/F_0$) were also less than half that of spontaneous $[Ca^{2+}]_i$ transient amplitudes (1.99 ± 0.34 $\Delta F/F_0$). Note: errors are reported as ± 1 S.E.M.

'instantaneous' firing frequencies. These were generated as the reciprocal of the inter-spike interval between the transient of interest and the subsequent transient. Peaks for transient probability data were determined by thresholding at a level five times the standard deviation of the baseline noise.

IR-triggered *versus* spontaneous fluorescence peak height comparisons were performed using cells with sufficiently slow (typically <0.5 Hz) spontaneous $[Ca^{2+}]_i$ transient ('transient') rates or with quiescent cells (no spontaneous transients) so that IR-triggered release could be clearly resolved from spontaneous release. DC drifts were removed through subtraction of a linear fit calculated from points in transient-free areas at the start and end of each set. IR-triggered peaks were subsequently identified by thresholding within a 1 s range of the trigger. Spontaneous peaks were identified through thresholding in regions outside of the IR pulsing periods.

Statistics

Summarized results are expressed as means and standard deviation (S.D.). Student's *t* test for paired data was used to compare the differences between groups of data with $P < 0.05$ considered to be statistically significant. Error bars in figures are representative of ± 1 standard error of the mean (S.E.M.).

Results

IR stimulation of sufficient intensity (>8.3 J cm^{-2}) consistently evoked transient $[Ca^{2+}]_i$ increases in viable cardiomyocytes. As shown in Fig. 1, the IR-evoked $[Ca^{2+}]_i$ events (Fig. 1*Aiii*) were distinguished from spontaneous $[Ca^{2+}]_i$ transients (Fig. 1*Aii* and Supplemental Material Movie 1) by their smaller amplitude and shorter time course. Another distinguishing feature of IR-evoked $[Ca^{2+}]_i$ events was the spatial uniformity and temporal synchrony of release across the cell body for IR-evoked events (Fig. 1*Aiii*), *vs.* the local $[Ca^{2+}]_i$ 'spark' release and $[Ca^{2+}]_i$ waves associated with spontaneous transients (Fig. 1*Aiv*). IR pulses evoked $[Ca^{2+}]_i$ events where the fluorescence increased above the background level (F_0) by 0.88 $\Delta F/F_0$ and recovered to the background level with a time constant of 0.64 s. This increase was sufficient to consistently induce contractile responses (Supplemental Material, Movie 2) in the cardiomyocytes. Within individual cells, differences in amplitude (Fig. 1*B*) and recovery time course (τ, Fig. 1*C*) for IR-evoked events *vs.* spontaneous transients were statistically significant ($P < 0.05$, *t* tests, $n = 21$). Overall the IR-evoked events exhibiting lower amplitudes (0.88 $\Delta F/F_0$ (S.D. 1.1) *vs.* 1.99 (S.D. 1.6) $\Delta F/F_0$) and faster recovery time constants (0.66 s (S.D. 0.67) *vs.* 1.19 s (S.D. 1.2)) compared to spontaneous

transients (Fig. 1*D*). Experimental limitations prevented us from quantifying fast onset kinetics of $[Ca^{2+}]_i$ transients.

Responses to individual IR pulses were dose dependent. As the IR energy per pulse was increased, the probability of evoking a $[Ca^{2+}]_i$ event for each IR pulse increased. One representative example is shown in Fig. 2*A* where the baseline $[Ca^{2+}]_i$ and the probability of evoking a $[Ca^{2+}]_i$ event both increased with IR dose. Fig. 2*B* provides the dose–response curve for a population of cells (indicated in parentheses), showing a half-maximal activation occurring at 6.3 J cm^{-2} pulse^{-1} and maximal activation at exposures greater than 8.3 J cm^{-2} pulse^{-1} (Fig. 2*B*). Comparison of IR-evoked $[Ca^{2+}]_i$ event amplitudes did not reveal any statistically significant correlation to the level of IR exposure. Changes in background $[Ca^{2+}]_i$ were sometimes observed at the higher radiant energy exposures (i.e. Fig. 2*A*, 9.1 J cm^{-2}).

IR-evoked $[Ca^{2+}]_i$ increases often triggered spontaneous transients, or led to trains of spontaneous transients, presumably through ryanodine receptor (RyR) mediated CICR. For quiescent cells, these transients could be entrained to the stimulation frequency of the laser, on a pulse-by-pulse basis, at rates of 1 Hz and below. Figure 3*A* shows one example of a quiescent cell that generated 'paced' $[Ca^{2+}]_i$ transients, triggered by individual IR pulses at 0.75 Hz and 10.3 J cm^{-2} pulse^{-1}. Following stimulation, spontaneous transients would frequently occur for several seconds, most probably due to an IR-evoked increase in the background intracellular

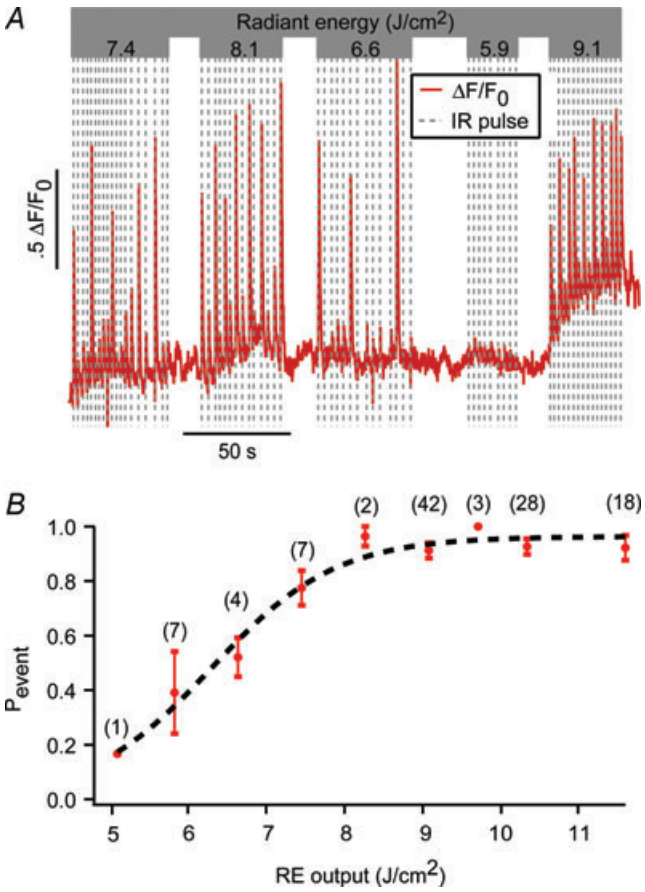

Figure 2. Activation thresholds for IR-evoked Ca^{2+} release
A, fluorescence intensity trace for a single neonatal cardiomyocyte exposed to varying radiant energy (RE) levels of IR. Release exhibited an all-or-nothing activation dependence with no consistent amplitude variability with RE. *B*, probability of $[Ca^{2+}]_i$ event (P_{event}) for each IR pulse (number of cells per point in parentheses) as a function of pulse RE. Data indicated that the activation threshold for IR-evoked release occurred in a sigmoidal fashion with RE with a half-maximal probability of activation occurring at 6.3 J cm^{-2} and maximal probability at REs >8.3 J cm^{-2}. Error bars indicate ±1 S.E.M.

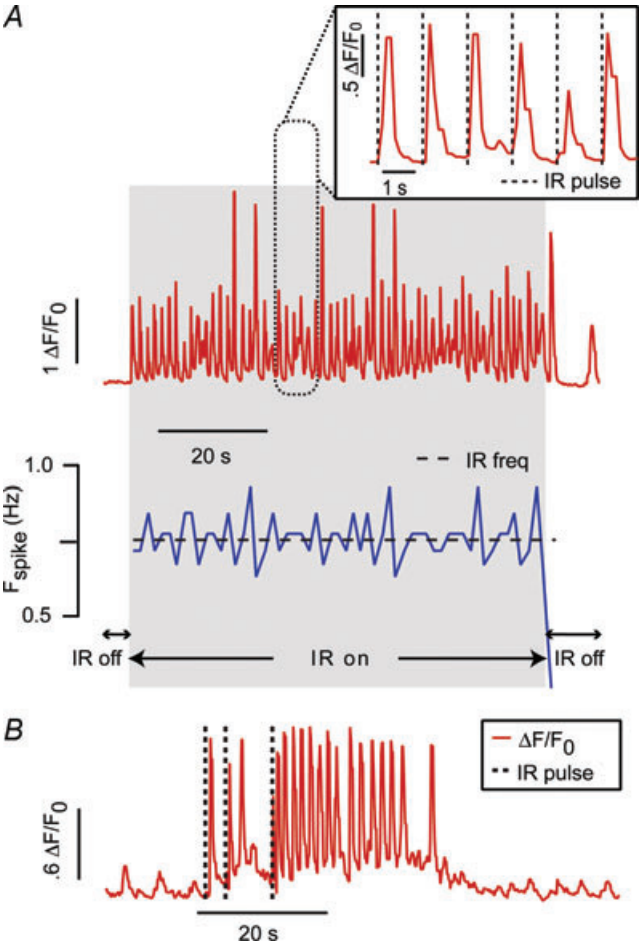

Figure 3. Quiescent cell responses
A, top trace shows the $[Ca^{2+}]_i$ fluorescence response for an isolated cardiomyocyte exposed to internally triggered IR (0.75 pulses s^{-1}, 10.3 J cm^{-2}). A close up (inset) shows the $[Ca^{2+}]_i$ transients follow IR stimulation in a one-to-one fashion and the instantaneous firing rate (blue/bottom trace) immediately syncs to that of the laser. *B*, following stimulation, spontaneous transients would frequently continue for several seconds. An example of this behaviour is shown here for a quiescent cell that was stimulated with three 11.6 J cm^{-2} IR pulses to initiate a brief period of spontaneous beating.

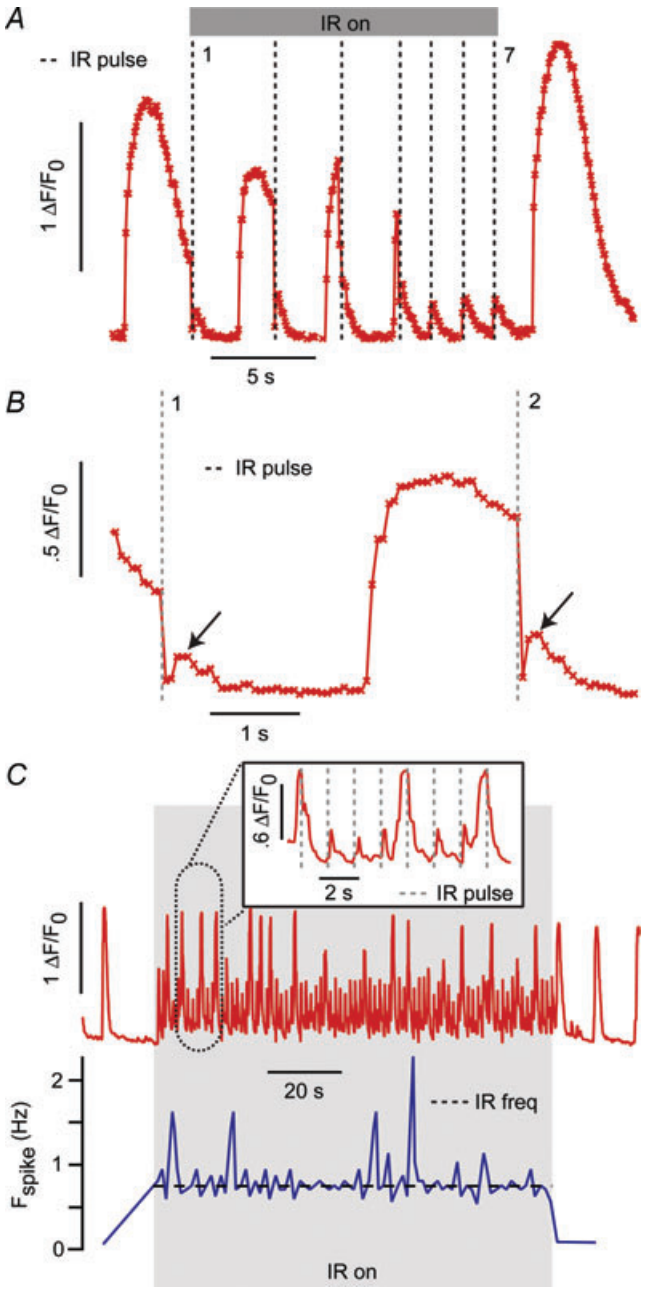

Figure 4. Spontaneously beating cell responses
A, the IR (1862 nm, 0.75 Hz, 9.1 J cm^{-2})-evoked $[Ca^{2+}]_i$ response depended on the timing of the IR pulse relative to the spontaneous Ca_i^{2+} release. As shown during pulses 1–4 (dashed lines), application during a spontaneous $[Ca^{2+}]_i$ transient resulted in abrupt $[Ca^{2+}]_i$ drops. Application during baseline $[Ca^{2+}]_i$ periods (pulses 5–7) resulted in transient $[Ca^{2+}]_i$ increases. *B*, a close-up view of pulses 1 and 2 reveals that, following the IR-evoked $[Ca^{2+}]_i$ drop, there is a subsequent rise, similar to the $[Ca^{2+}]_i$ transients witnessed during baseline $[Ca^{2+}]_i$ periods. *C*, the overall $[Ca^{2+}]_i$ kinetics could still be entrained to the pulse frequency of the laser (on-period is in shaded grey area, red/top trace is the fluorescence intensity, bottom/blue trace is the instantaneous spike frequency). As seen in the inset, while the subthreshold transients could trigger the onset of a spontaneous transient, it would be truncated by the subsequent IR pulse, thereby maintaining pulse synchrony.

$[Ca^{2+}]_i$. An example of this behaviour is shown in Fig. 3*B* for a quiescent cell that was stimulated with three 11.6 J cm^{-2} IR pulses to initiate a train of spontaneous $[Ca^{2+}]_i$ transients.

Application of pulsed IR during a period of a spontaneous $[Ca^{2+}]_i$ transient did not alter the IR-evoked $[Ca^{2+}]_i$ event, but did reveal a fast component that was not observable for stimuli delivered at resting $[Ca^{2+}]_i$. Figure 4 is a representative record showing very fast reductions in $[Ca^{2+}]_i$ immediately upon application of the IR pulse, followed by the IR-evoked $[Ca^{2+}]_i$ event described above. The IR-evoked $[Ca^{2+}]_i$ increases were the same for all pulses (Fig. 4*A*, 1–7), but preceded by a rapid decrease in $[Ca^{2+}]_i$ when tested during elevated $[Ca^{2+}]_i$. The decrease rapidly restored $[Ca^{2+}]_i$ to approximately the baseline level (Fig. 4*B*, vertical dashed lines), just prior to the appearance of the IR-evoked event (Fig. 4*B*, arrows). We were unable to resolve the time course of the fast transient due to limitations of the instrumentation, but the response was clearly faster than the sampling rate of 129 ms. Since the fast IR response reset the $[Ca^{2+}]_i$ to roughly the baseline level, it also altered the timing of spontaneous transients. One example of this is shown in Fig. 4*C* as the instantaneous spike frequency (Fig. 4*C*, blue trace) synchronized to the 0.75 Hz laser pulse frequency (Fig. 4*C*, dashed line) for the duration of the IR pulsing. The inset highlights a representative epoch where relatively small IR-evoked events entrained the spontaneous timing by truncation of spontaneous $[Ca^{2+}]_i$ transients. Finally, in a small subset of cells (<5%), IR stimulation did not result in observable pulse-for-pulse $[Ca^{2+}]_i$ events. In these cases, laser stimulation would increase the spontaneous $[Ca^{2+}]_i$ transient frequency without a detectable IR-evoked $[Ca^{2+}]_i$ event (not shown).

Myocytes were challenged with pharmacological agents to identify the potential intracellular contributors to the IR-evoked response. The application of Ryanodine (100 μM) did not eliminate the IR-evoked response ($n = 8$). While Ryanodine did not block the transient altogether, it did significantly ($P < .02$, *t* test) decrease the IR-evoked $[Ca^{2+}]_i$ event amplitude from 0.90 $\Delta F/F_0$ (S.D. 0.34) to 0.25 $\Delta F/F_0$ (S.D. 0.18, $n = 8$) for the pre-drug treated cells *versus* the ryanodine-treated cells, respectively (Fig. 5*A*).

Three compounds did prove to be potent inhibitors of the IR-evoked $[Ca^{2+}]_i$ response: (1) CGP-37157 (20 μM, $n = 12$, $k = 12$ blocked), a known inhibitor of mitochondrial Na^+/Ca^{2+} exchanger (mNCX), and (2) Ruthenium Red (40 μM, $n = 13$, $k = 10$) an inhibitor of the mitochondrial Ca^{2+} uniporter (mCU), and (3) 2-aminoethoxydiphenylborane (2-APB; 10 μM, $n = 6$ cells, $k = 4$), an IP_3 channel antagonist. Example washout data for these three compounds are shown in Fig. 5*C* and *D*. The results show the pre-drug $[Ca^{2+}]_i$ response, the response following 10–15 min exposure to

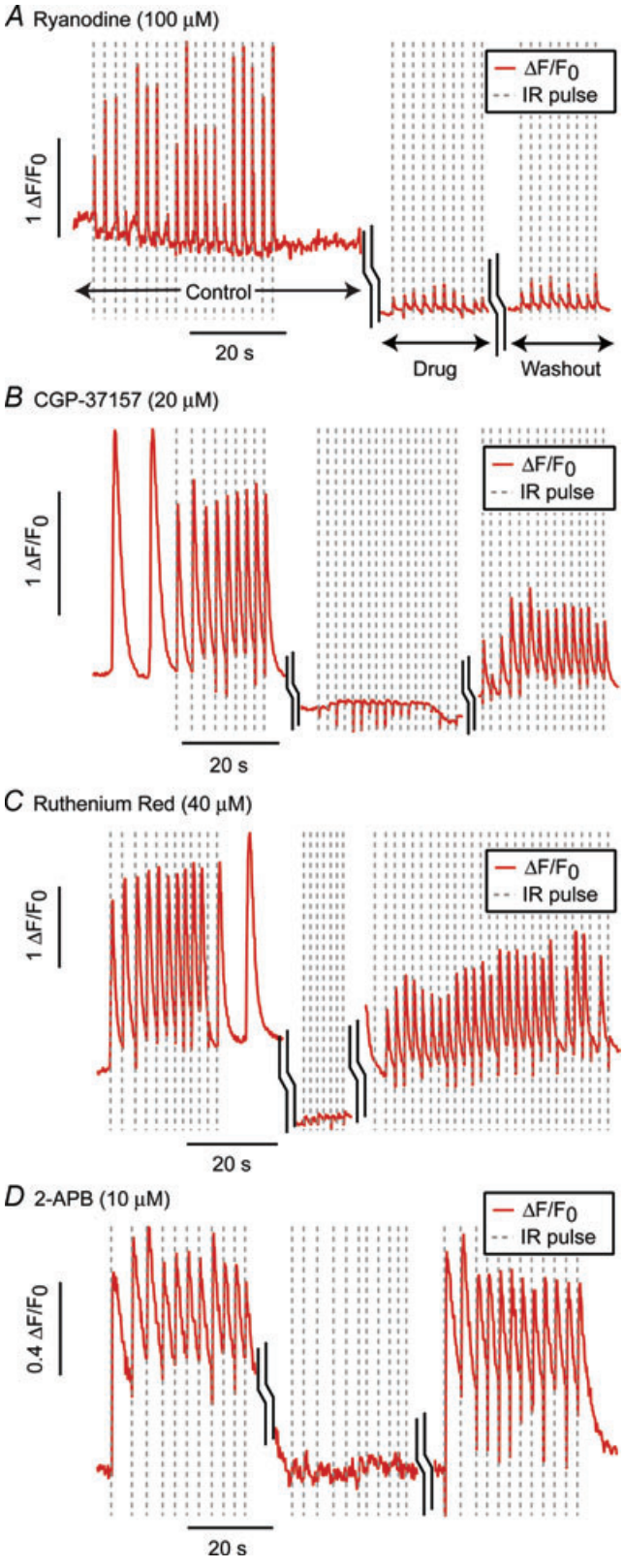

Figure 5. Pharmacology
Representative data for application of ryanodine (100 μM, $n = 6$ cells), an RyR channel antagonist (at this concentration) (*A*), CGP-37157 (20 μM, $n = 12$), a known inhibitor of mNCX (*B*), Ruthenium Red (40 μM, $n = 13$) an inhibitor of mCU (*C*), and 2-APB (10 μM, $n = 6$), an IP_3 channel antagonist (*D*). Each graph is a composite of the pre-drug cell $[Ca^{2+}]_i$ fluorescence response ('control'), the response following 10–15 min exposure to the drug ('drug'), and the response after 4× washout of the drug. ('washout') as labelled in *A*.

the drug, and the response after 4× washout of the drug. In the case of CGP-37157 and Ruthenium Red, the washout IR-evoked event was often diminished relative to the pre-drug response. Additionally, in some sets, negative transients were witnessed (examples in Figs 2*A* and Fig. 5*B*) that could potentially be undersampled fast negative transients similar to those shown in Fig. 4*B* but occurring during baseline $[Ca^{2+}]_i$ phases thereby resulting in a drop below the initial baseline fluorescence.

Discussion

IR-evoked $[Ca^{2+}]_i$ transients

Pulsed IR in the 1862 nm wavelength range was demonstrated to be effective at stimulating neonatal rat ventricular cardiomyocytes. The IR-evoked response included $[Ca^{2+}]_i$ events and observed mechanical contractions (Supplemental Material, Movie 2). IR-evoked $[Ca^{2+}]_i$ events were distinguishable from spontaneous $[Ca^{2+}]_i$ transients and Ca^{2+} sparks associated with spontaneous beating in their decreased amplitude, faster recovery time constant, and uniformity of release throughout the cell (Fig. 1 and Movie 1). These factors were initial indications of $[Ca^{2+}]_i$ release distinct from sarcolemmal L-type Ca^{2+} channel currents and RyR channel release from SR. Upon fitting the exponential decay of both types of transients, the IR-evoked decay occurred at a statistically significant, faster rate than the spontaneous one ($\tau = 0.66$ s *vs.* 1.19 s). As the rate of Ca^{2+} uptake kinetics has been previously reported to have a direct correlation to the peak level of the spontaneous $[Ca^{2+}]_i$ transient (Bers & Berlin, 1995), the faster recovery of IR-evoked events *vs.* spontaneous transients suggests another mechanism is decreasing τ during stimulation. We speculate that this change in τ results from the recently depleted source of the IR-evoked release providing an up-regulated sink for Ca^{2+} uptake relative to standard conditions.

Energy dependence of IR-evoked response

The IR-evoked response exhibited a direct energy dependence with a threshold of ~6.3 J cm^{-2} for half-maximal activation and greater than 8.3 J cm^{-2} for maximal activation (Fig. 2). This is significantly higher than that reported to excite action potentials in rat sciatic

nerve (0.312–1.22 J cm^{-2}) (Wells *et al.* 2005) and auditory cells (1.6–15.1 mJ cm^{-2}) (Izzo *et al.* 2006). However, the average power for maximal activation in this study (10.38 mW) was similar to that previously reported (15–30 mW) for 780 nm pulsed IR stimulation of cardiomyocytes (Smith *et al.* 2008). As prior studies have strongly implicated thermal activation in the response of other cells to pulsed IR lasers (Wells *et al.* 2007; Tseeb *et al.* 2009), the sigmoidal activation curve (Fig. 2*B*) was not surprising. However, once threshold was attained, there was no consistent, empirical difference in the magnitude of the $[Ca^{2+}]_i$ events. This result excludes passive, intracellular protein buffers as the principle effectors in that they would expectedly exhibit wider activation with energy, as opposed to the all or nothing responses witnessed here. In addition to IR-evoked $[Ca^{2+}]_i$ events, there was a noticeable baseline increase in $[Ca^{2+}]_i$ at higher radiant energy levels. This did not fluctuate with the IR pulse frequency and is presumably due to the increased Ca^{2+} load imposed on $[Ca^{2+}]_i$ regulatory mechanisms.

Quiescent cell response

As with IR stimulation of other cell types (Izzo *et al.* 2006; Wells *et al.* 2007; Rajguru *et al.* 2011), we found that IR-triggered events could be 'paced' or synchronized to the IR stimulus. In quiescent cells the $[Ca^{2+}]_i$ response immediately matched the IR stimulus with a one-to-one correspondence of $[Ca^{2+}]_i$ events to IR pulses (Fig. 3*A*). There were occasional 'missed' transients attributed to incomplete Ca^{2+} loading. IR-evoked events would also periodically trigger the larger spontaneous $[Ca^{2+}]_i$ transients (Fig. 3*A*. large transients, Fig. 3*B*) typically associated with ECC in cardiomyocytes. Given the CICR underpinnings of ECC, this is not a surprising result. The failure to evoke a spontaneous $[Ca^{2+}]_i$ event for each IR evoked event is likely attributable to the immaturity of the CICR system in neonatal myocytes which lack the highly-ordered T-Tubule networks present in their adult counterparts (Korhonen *et al.* 2009).

Spontaneously beating cell response

In spontaneously beating cells, the IR response was more complex. Application of pulsed IR during a period of a spontaneous $[Ca^{2+}]_i$ transient did not alter the IR-evoked $[Ca^{2+}]_i$ event, but did reveal a fast component that was not observable for stimuli delivered at resting $[Ca^{2+}]_i$. IR triggered an abrupt cessation of the spontaneous $[Ca^{2+}]_i$ transient and a rapid decrease in the $[Ca^{2+}]_i$ signal, often returning it close to baseline $[Ca^{2+}]_i$ levels. Following this drop, a small transient rise, identical to the IR-evoked $[Ca^{2+}]_i$ rise occurred (Fig. 4*B*, arrows). These results indicate that the magnitude of the Ca^{2+} clearance (negative response) was highly dependent on the cytosolic $[Ca^{2+}]_i$. This raised the possibility of the participation of mCU which has been estimated to have a $[Ca^{2+}]_i$ threshold of 500 nM required for initiation of Ca^{2+} influx (Miyata *et al.* 1991). As the resting $[Ca^{2+}]_i$ in neonatal cardiomyocytes has been estimated to be ∼100 nM (Bers, 2001), increasing the open probability of mCU during baseline $[Ca^{2+}]_i$ periods would have a much smaller effect on $[Ca^{2+}]_i$ than would a similar increase during spontaneous $[Ca^{2+}]_i$ transient periods, as is consistent with our data. As a result, this negative transient might be present during IR-evoked events in baseline $[Ca^{2+}]_i$ periods but might not be readily discernable from the baseline noise or resolvable with our 129 ms sampling rate. Supporting this notion, we did occasionally detect IR-evoked negative $[Ca^{2+}]_i$ transients during baseline $[Ca^{2+}]_i$ periods (examples in Fig. 2*A*, Fig. 5*B*). IR interaction with mitochondria would also concomitantly result in increased activity of mNCX, possibly explaining the IR-evoked transient increases in $[Ca^{2+}]_i$ that occur during stimulation in both spontaneous $[Ca^{2+}]_i$ transient and rest periods. Despite the increased complexity of the spontaneous cell response, the timing dependent behaviour still allowed these cells to be paced by IR (as shown in Fig. 4*C*) by truncating, or phase-advancing, the spontaneous $[Ca^{2+}]_i$ transients.

In a third, smaller subset of spontaneously beating cells, the IR did not generate observable $[Ca^{2+}]_i$ events but did slowly increase the rate of spontaneous firing evidence that IR-evoked $[Ca^{2+}]_i$ changes were present. For some cases, we speculate that responses might have been primarily due to heating and indirect/partial illumination of the cell with IR. This idea is corroborated by experimental data showing differences between indirect heating and direct IR stimulation (Rajguru *et al.* 2011).

Pharmacological studies

Given its prominent role in CICR in cardiomyocytes and its thermosensitivity (Feliciano Protasi *et al.* 2004), it might be anticipated that the source for IR-evoked $[Ca^{2+}]_i$ release would be from SR through RyR channels. To test that hypothesis, we applied ryanodine to the cells at the 100 μM concentration that is known to block these channels in cardiomyocytes (Meissner, 1986). Surprisingly, it did not entirely block the $[Ca^{2+}]_i$ response but instead only diminished its amplitude (Fig. 5*A*), suggesting an indirect contribution of RyR release to the overall IR-evoked $[Ca^{2+}]_i$ response.

Pharmacological compounds were applied to evaluate the role of mitochondria in IR-evoked $[Ca^{2+}]_i$ responses. Both CGP-37157 (a specific inhibitor of mNCX) and Ruthenium Red (an inhibitor of mCU) reversibly blocked the IR-evoked response (Fig. 5*B* and *C*). Although

washout of the drugs did not restore the full amplitude of the IR-evoked $[Ca^{2+}]_i$ response, this could be attributable to residual effects due to an inability to completely wash the drug out of the cytoplasm as has been shown with other compounds in cardiomyocytes (Escobar *et al.* 2004). Overall, these results implicate mitochondria as the major intracellular store of Ca^{2+} involved in IR-evoked cytosolic changes in $[Ca^{2+}]_i$. The results are also consistent with prior work demonstrating the strong buffering capabilities of myocytes and beat-to-beat fluctuations of mitochondrial Ca^{2+} (Robert *et al.* 2001; Seguchi *et al.* 2005). Mitochondrial Ca^{2+} flux is also consistent with the spatial homogeneity of IR-evoked $[Ca^{2+}]_i$ events in that neonatal cardiomyoctes have been shown to form an interconnected 'mitochondrial reticulum' spanning the cell (Griffiths *et al.* 2010). Furthermore, the high K_d of mCU Ca^{2+} activation would create a concentration dependence consistent with results in Fig. 4.

Evidence in HeLa cells (Tseeb *et al.* 2009) indicated IP_3 receptors play a role in heat pulse-evoked $[Ca^{2+}]_i$ events. Since IP_3 coupling to ECC has been demonstrated in adult ventricular cardiomyocytes (Domeier *et al.* 2008), we examined the effects of 2-APB, an IP_3-channel antagonist. Results were positive and suggest the involvement of the IP_3 in IR-evoked $[Ca^{2+}]_i$ events (Fig. 5*D*). In light of the mitochondrial response, this 2-APB result might be a secondary effect of the drug given that high 2-APB concentrations has been reported to inhibit mitochondrial Ca^{2+} efflux in Jurkat T-cells (Prakriya & Lewis, 2001).

A second possibility for the effect of 2-APB, which is consistent with the mitochondrial results, might involve $[Ca^{2+}]_i$ microdomain formation. Evidence in HeLa cell clones has shown that high $[Ca^{2+}]_i$ microdomains are created from Ca^{2+} release through IP_3 channels that were proposed to be juxtapositioned to mCU channels (Rizzuto *et al.* 1993). This has been postulated as a means of activating mCU in spite of its high K_d (Miyata *et al.* 1991; Griffiths *et al.* 2010) and might explain sensitivity to 2-APB in the present study. Ultrastructural, Ca^{2+} buffering, and mitochondrial Ca^{2+} imaging studies have all supported the hypothesis of Ca^{2+} communication between SR and mitochondria in gaps smaller than 15 nm (Sharma *et al.* 2000; Szalai *et al.* 2000; Parfenov *et al.* 2006; Lukyanenko *et al.* 2009). However, to date, all evidence has indicated transmission from RyR channels (not IP_3 channels) to mCU. In the context of our results, the microdomain formation during spontaneous $[Ca^{2+}]_i$ transients would support the hypothesis of mCU underlying the timing-dependent IR-evoked $[Ca^{2+}]_i$ response and overall mitochondrial activation. A caveat is that, to our knowledge, the relative spatial proximity of RyR and mitochondria in neonatal cardiomyocytes is unknown. It is also possible, given the presence of IP_3 receptors in cardiomyocyte SR (Domeier *et al.* 2008), that there is a Ca^{2+} communication between IP_3 channels and mitochondria.

Mitochondrial involvement in the IR-evoked response

Taken as a whole, these data point strongly towards mitochondria as the primary facilitator of IR-evoked $[Ca^{2+}]_i$ events in neonatal cardiomyocytes. The specific involvement of both mCU and mNCX implies that the cellular response to IR results from either (1) a whole organelle/mitochondria effect that simultaneously activates and/or increases the rate constants of both channels or (2) a direct effect of IR on the mCU (or possibly rapid mode of Ca^{2+} uptake into mitochondria) thereby inducing rapid Ca^{2+} uptake that subsequently results in an mNCX Ca^{2+} efflux to restore the electrochemical equilibrium. Given the relative timing of the two effects (Fig. 4*A* and *B*), as coarsely resolved by our set-up, we would speculate that the latter case is the most probable. Although, the recent identification of a Letm1 Ca^{2+}/H^+ antiporter in mitochondria that is sensitive to both Ruthenium Red and CGP-37157 raises the additional possibility of its involvement in the IR-evoked response as well and merits further investigation (Jiang *et al.* 2009). Results indicate an indirect contribution to release from the RyR, through Ca^{2+} loading of the mitochondria and/or through CICR following mitochondrial Ca^{2+} efflux. With our current experimental setup, we were not able to resolve the sequence of these processes. A future area of exploration is to determine the underlying biophysical mechanism(s) of IR-evoked uptake and release. Earlier studies have pointed towards the prominent role of heating in IR-evoked release (Wells *et al.* 2007; Tseeb *et al.* 2009). Our finding of preferential mitochondrial release of Ca^{2+} suggests that there is a greater sensitivity for the mitochondria relative to other intracellular Ca^{2+} stores. In a historical context, this is not a surprising result as the role of mitochondria as the primary chromophore in photobiological responses in cells has long been established with the putative chromophore for longer wavelength mitochondrial absorption being the enzyme cytochrome *c* oxidase (COX) (Chance & Hess, 1959; Salet, 1972; Salet *et al.* 1976, 1979; Lavi *et al.* 2010). While studies of the effects of light radiation on mitochondria at other wavelengths have demonstrated photochemical reduction of COX (Karu *et al.* 2005) as well as mitochondrial reactive oxygen species generation (Callaghan *et al.* 1996; Grossman *et al.* 1998; Hockberger *et al.* 1999; Alexandratou *et al.* 2002; Hirase *et al.* 2002; Lavi *et al.* 2003). In general the time course of these processes would appear to be too slow to underlie the effects witnessed in this study (Callaghan *et al.* 1996; Alexandratou *et al.* 2002; Lavi *et al.* 2003; Karu *et al.* 2005). To our knowledge, no data exist for mitochondrial absorption at the specific

wavelength used in the present study (1862 nm). Overall, given the speed and reversibility of the IR-evoked response as well as the broad effects on both mitochondrial Ca^{2+} uptake and release, conversion of the electromagnetic energy in the IR to heat is the most likely effector.

TRP channel involvement

Yet another possibility for IR-triggered stimulation is the involvement of transient receptor potential (TRP) channels such as the thermosensitive TRPV subfamily. Consistent with that hypothesis would be the generic effects that both 2-APB and Ruthenium Red have been shown to have in blocking such receptors (Szallasi & Blumberg, 1999; Xu *et al.* 2005). Additionally, the baseline increase in $[Ca^{2+}]_i$ at high radiant energy levels (Fig. 2*A*) is also compatible with such temperature-dependent activation. However, removal of extracellular Ca^{2+} did not affect the generation of Ca^{2+} waves resulting from IR (780 nm) stimulation of HeLA cells, making TRP channel involvement unlikely in that case (Smith *et al.* 2001). Additionally, unlike the mitochondrial-activation hypothesis, TRP channel involvement does not account for the effects of CGP-37157. Consequently, given all three compounds have demonstrated inhibition of mitochondrial Ca^{2+} flux, IR-evoked mitochondrial mCU and mNCX activation is the most viable hypothesis for the rapid $[Ca^{2+}]_i$ transients. However, given the thermosensitivity of TRP channels and the known bulk temperature changes related to IR stimulation, we would expect a pronounced contribution from TRP channels in cells in which these are highly expressed. Further investigation of potential sarcolemmal contributors is warranted.

Conclusions

With the recent prominence that mitochondrial Ca^{2+} storage and release has assumed in biophysical studies of cardiomyocytes, IR-based stimulation of mitochondrial Ca^{2+} cycling might provide a valuable tool for studying its role in ECC and $[Ca^{2+}]_i$ buffering. As we are not aware of any available mNCX agonist or stimulation approach, this technique could provide the first direct mechanism for enhancing mNCX activation. Additionally, IR has the potential to supplement the existing agonists of mCU activity (Nicchitta & Williamson, 1984; Montero *et al.* 2004). Furthermore, as respiration in mitochondria has been linked to mitochondrial calcium cycling (McCormack & Denton, 1993), IR stimulation at 1862 nm wavelength could potentially provide an exogenous approach for controlling the oxidative metabolism in cells as has been reported for irradiation at lower wavelengths (Yu *et al.* 1997). A valuable feature of IR stimulation is that activation can be accomplished without the need for permeabilizing the cell membrane or piercing the cell with a micropipette. However, prior to use in these applications, the biophysical underpinnings may need to be elucidated, including the roles of RyR and IP_3 receptors in IR-evoked release. Furthermore, because of the heterogeneous, constantly evolving nature of cytosolic Ca^{2+} signals in the neonatal cardiomyocyte (Escobar *et al.* 2004), conclusions drawn from this work are difficult to extrapolate to adult cardiomyocyte function or to other cell lines. Future experiments will need to focus on the more stable properties of the adult cardiomyocytes for a better understanding of relative contributions of all cellular components to IR-triggered events.

References

Alexandratou E, Yova D, Handris P, Kletsas D & Loukas S (2002). Human fibroblast alterations induced by low power laser irradiation at the single cell level using confocal microscopy. *Photochem Photobiol Sci* **1**, 547–552.

Ando J, Smith NI, Fujita K & Kawata S (2009). Photogeneration of membrane potential hyperpolarization and depolarization in non-excitable cells. *Eur Biophys J* **38**, 255–262.

Arvanitaki A & Chalazonitis N (1961). Excitatory and inhibitory processes initiated by light and infra-red radiation in single identifiable nerve cells. In *Nervous Inhibition: Proceedings of the Second Friday Harbor Symposium*, ed. Florey E, pp. 194–231. Pergamon Press, Seattle, WA.

Bers DM (2001). *Excitation-Contraction Coupling and Cardiac Contractile Force*. Kluwer Academic Publishers, Boston, MA.

Bers DM (2008). Calcium cycling and signaling in cardiac myocytes. *Annu Rev Physiol* **70**, 23–49.

Bers DM & Berlin JR (1995). Kinetics of $[Ca]_i$ decline in cardiac myocytes depend on peak $[Ca]_i$. *Am J Physiol Cell Physiol* **268**, C271–C277.

Callaghan GA, Riordan C, Gilmore WS, McIntyre IA, Allen JM & Hannigan BM (1996). Reactive oxygen species inducible by low-intensity laser irradiation alter DNA synthesis in the haemopoietic cell line U937. *Lasers Surg Med* **19**, 201–206.

Cannell MB, Berlin JR & Lederer WJ (1987). Intracellular calcium in cardiac myocytes: Calcium transients measured using fluorescence imaging. *Soc Gen Physiol Ser* **42**, 201–214.

Chance B & Hess B (1959). Spectroscopic evidence of metabolic control. *Science* **129**, 700–708.

Domeier TL, Zima AV, Maxwell JT, Huke S, Mignery GA & Blatter LA (2008). IP3 receptor-dependent Ca^{2+} release modulates excitation-contraction coupling in rabbit ventricular myocytes. *Am J Physiol Heart Circ Physiol* **294**, H596–H604.

Drummond GB (2009). Reporting ethical matters in *The Journal of Physiology*: standards and advice. *J Physiol* **587**, 713–719.

Escobar AL, Ribeiro-Costa R, Villalba-Galea C, Zoghbi ME, Perez CG & Mejıa-Alvarez R (2004). Developmental changes of intracellular Ca^{2+} transients in beating rat hearts. *Am J Physiol Heart Circ Physiol* **286**, H971–H978.

Protasi F, Shtifman A, Julian FJ & Allen PD (2004). All three ryanodine receptor isoforms generate rapid cooling responses in muscle cells. *Am J Physiol Cell Physiol* **286**, C662–670.

Fink C, Ergun S, Kralisch D, Remmers U, Weil J & Eschenhagen T (2000). Chronic stretch of engineered heart tissue induces hypertrophy and functional improvement. *FASEB J* **14**, 669–679.

Griffiths EJ, Balaska D & Cheng WHY (2010). The ups and downs of mitochondrial calcium signalling in the heart. *Biochim Biophys Acta* **1797**, 856–864.

Grossman N, Schneid N, Reuveni H, Halevy S & Lubart R (1998). 780 nm low power diode laser irradiation stimulates proliferation of keratinocyte cultures: involvement of reactive oxygen species. *Lasers Surg Med* **22**, 212–218.

Hirase H, Nikolenko V, Goldberg JH & Yuste R (2002). Multiphoton stimulation of neurons. *J Neurobiol* **51**, 237–247.

Hockberger PE, Skimina TA, Centonze VE, Lavin C, Chu S, Dadras S, Reddy JK & White JG (1999). Activation of flavin-containing oxidases underlies light-induced production of H_2O_2 in mammalian cells. *Proc Natl Acad Sci U S A* **96**, 6255–6260.

Iwanaga S, Kaneko T, Fujita K, Smith N, Nakamura O, Takamatsu T & Kawata S (2006). Location-dependent photogeneration of calcium waves in HeLa cells. *Cell Biochem Biophys* **45**, 167–176.

Izzo AD, Richter C-P, Jansen ED & Walsh JT (2006). Laser stimulation of the auditory nerve: Effect of shorter pulse duration and penetration depth. *Biophys J* **94**, 3159–3166.

Jenkins MW, Duke AR, Gu S, Doughman Y, Chiel HJ, Fujioka H, Watanabe M, Jansen ED & Rollins AM (2010). Optical pacing of the embryonic heart. *Nat Photonics* **4**, 623–626.

Jiang D, Zhao L & Clapham DE (2009). Genome-wide RNAi screen identifies Letm1 as a mitochondrial Ca^{2+}/H^{+} antiporter. *Science* **326**, 144–147.

Karu TI, Pyatibrat LV, Kolyakov SF & Afanasyeva NI (2005). Absorption measurements of a cell monolayer relevant to phototherapy: Reduction of cytochrome c oxidase under near IR radiation. *J Photochem Photobiol B* **81**, 98–106.

Korhonen T, Hanninen SL & Tavi P (2009). Model of excitation-contraction coupling of rat neonatal ventricular myocytes. *Biophys J* **96**, 1189–1209.

Lavi R, Shainberg A, Friedmann H, Shneyvays V, Rickover O, Eichler M, Kaplan D & Lubart R (2003). Low energy visible light induces reactive oxygen species generation and stimulates an increase of intracellular calcium concentration in cardiac cells. *J Biol Chem* **278**, 40917–40922.

Lavi R, Shainberg A, Shneyvays V, Hochauser E, Isaac A, Zinman T, Friedmann H & Lubart R (2010). Detailed analysis of reactive oxygen species induced by visible light in various cell types. *Lasers Surg Med* **42**, 473–480.

Lukyanenko V, Chikando A & Lederer WJ (2009). Mitochondria in cardiomyocyte Ca^{2+} signaling. *Int J Biochem Cell Biol* **41**, 1957–1971.

McCormack JG & Denton RM (1993). Mitochondrial Ca^{2+} transport and the role of intramitochondrial Ca^{2+} in the regulation of energy metabolism. *Dev Neurosci* **15**, 165–173.

Meissner G (1986). Ryanodine activation and inhibition of the Ca^{2+} release channel of sarcoplasmic reticulum. *J Biol Chem* **261**, 6300–6306.

Miyata H, Silverman HS, Sollott SJ, Lakatta EG, Stern MD & Hansford RG (1991). Measurement of mitochondrial free Ca^{2+} concentration in living single rate cardiac myocytes. *Am J Physiol Heart Circ Physiol* **261**, H1123–H1134.

Montero M, Loabaton CD, Hernandez-Sanmiguel E, Santodomingo J, Vay L, Moreno A & Alvarez J (2004). Direct activation of the mitochondrial calcium uniporter by natural plant flavonoids. *Biochem J* **384**, 19–24.

Nicchitta CV & Williamson JR (1984). Spermine – a regulation of mitochondrial calcium cycling. *J Biol Chem* **259**, 12978–12983.

Parfenov AS, Salnikov V, Lederer WJ & Lukyanenko V (2006). Aqueous diffusion pathways as a part of the ventricular cell ultrastructure. *Biophys J* **90**, 1107–1119.

Prakriya M & Lewis RS (2001). Potentiation and inhibition of Ca^{2+} release-activated Ca^{2+} channels by 2-aminoethyldiphenyl borate (2-APB) occurs independently of IP_3 receptors. *J Physiol* **536**, 3–19.

Rajguru SM, Matic AI, Robinson AM, Fishman AJ, Moreno LE, Bradley A, Vujanovic I, Breen J, Wells JD, Bendett M & Richter C-P (2010). Optical cochlear implants: Evaluation of surgical approach and laser parameters in cats. *Hear Res* **269**, 102–111.

Rajguru SM, Richter C-P, Matic AI, Holstein GR, Highstein SM & Rabbitt RD (2011). Infrared photostimulation of the crista ampullaris. *J Physiol* **589**, 1283–1294.

Rizzuto R, Brini M, Murgia M & Pozzan T (1993). Microdomains with high Ca^{2+} close to IP_3-sensitive channels that are sensed by neighboring mitochondria. *Science* **262**, 744–747.

Robert V, Gurlini P, Tosello V, Nagai T, Miyawaki A, Lisa FD & Pozzan T (2001). Beat-to-beat oscillations of mitochondrial $[Ca^{2+}]$ in cardiac cells. *EMBO J* **20**, 4998–5007.

Salet C (1972). A study of beating frequency of a single myocardial cell I. Q-switched laser microirradiation of mitochondria. *Exp Cell Res* **73**, 360–366.

Salet C, Moreno G & Vinzens F (1976). A study of beating frequency of a single myocardial cell II. Ultraviolet micro-irradiation of the nucleus and of the cytoplasm. *Exp Cell Res* **100**, 365–373.

Salet C, Moreno G & Vinzens F (1979). A study of beating frequency of a single myocardial cell III. Laser micro-irradiation of mitochondria in the presence of KCN or ATP. *Exp Cell Res* **120**, 25–29.

Seguchi H, Ritter M, Shizukuishi M, Ishida H, Chokoh G, Nakazawa H, Spitzer KW & Barry WH (2005). Propagation of Ca^{2+} release in cardiac myocytes: Role of mitochondria. *Cell Calcium* **38**, 1–9.

Sharma VK, Ramesh V, Franzini-Armstrong C & Sheu S-S (2000). Transport of Ca^{2+} from sarcoplasmic reticulum to mitochondria in rat ventricular myocytes. *J Bioenerg Biomembr* **32**, 97–104.

Smith NI, Fujita K, Kaneko T, Katoh K, Nakamura O & Kawata S (2001). Generation of calcium waves in living cells by pulsed-laser-induced photodisruption. *Appl Phys Lett* **79**, 1208–1210.

Smith NI, Iwanaga S, Beppu T, Fujita K, Nakamura O & Kawata S (2006). Photostimulation of two types of Ca^{2+} waves in rat pheochromocytoma PC12 cells by ultrashort pulsed near-infrared laser irradiation. *Laser Phys Lett* **3**, 154–161.

Smith NI, Kumamoto Y, Iwanaga S, Ando J, Fujita K & Kawata S (2008). A femtosecond laser pacemaker for heart muscle cells. *Opt Express* **16**, 8604–8616.

Szalai G, Csordás G, Hantash BM, Thomas AP & Hajnóczky G (2000). Calcium signal transmission between ryanodine receptors and mitochondria. *J Biol Chem* **275**, 15305–15313.

Szallasi A & Blumberg PM (1999). Vanilloid (capsaicin) receptors and mechanisms. *Pharmacol Rev* **51**, 159–212.

Tseeb V, Suzuki M, Oyama K, Iwai K & Ishiwata Si (2009). Highly thermosensitive Ca^{2+} dynamics in HeLa cell through IP_3 receptors. *HFSP J* **3**, 117–123.

Wells J, Kao C, Jansen ED, Konrad P & Mahadevan-Jansen A (2005). Application of infrared light for in vivo neural stimulation. *J Biomed Opt* **10**, 1–11.

Wells J, Kao C, Konrad P, Milner T, Kim J, Mahadevan-Jansen A & Jansen ED (2007). Biophysical mechanisms of transient optical stimulation of peripheral nerve. *Biophys J* **93**, 2567–2580.

Xu S-Z, Zeng F, Boulay G, Grimm C, Harteneck C & Beech DJ (2005). Block of TRPC5 channels by 2-aminoethoxydiphenyl borate: A differential, extracellular and voltage-dependent effect. *Br J Pharmacol* **145**, 405–414.

Yu W, Naim JO, McGowan M, Ippolito K & Lamafame RJ (1997). Photomodulation of oxidative metabolism and electron chain enzymes in rat liver mitochondria. *Photochem Photobiol* **66**, 866–871.

Zhao Y, Zhang Y, Liu X, Lv X, Zhou W, Luo Q & Zeng S (2009). Photostimulation of astrocytes with femtosecond laser pulses. *Opt Express* **17**, 1291–1298.

Author contributions

G.M.D., S.M.R. and R.D.R were responsible for conception, design of this study and experiments. R.A.L. and R.W.H. performed cardiomyocyte isolations. G.M.D. and R.D.R. analysed the data and primarily wrote the manuscript. S.M.R., R.A.L. and R.W.H. contributed to the writing of the manuscript and provided critical review of the manuscript. All authors approved the final version of the manuscript.

Acknowledgements

The authors would like to thank Dr Ken Spitzer and Dr Steve Poelzing for sharing their expertise on cardiomyocytes and for their input in reviewing this manuscript; Dr Claus Peter-Richter for initial resource support and collaboration; Dr Patrick Tresco and the members of the Keck Lab of the University of Utah for use of their cell culture facilities; and Dr Stephen Highstein and Dr Holly Holman for valuable input in reviewing this manuscript. Funding sources: NIH R01DC006685 and R01 DC004928.